

NASA/TM—2001-210979



# Optimization of Training Sets for Neural-Net Processing of Characteristic Patterns From Vibrating Solids

Arthur J. Decker  
Glenn Research Center, Cleveland, Ohio

---

July 2001

## The NASA STI Program Office . . . in Profile

Since its founding, NASA has been dedicated to the advancement of aeronautics and space science. The NASA Scientific and Technical Information (STI) Program Office plays a key part in helping NASA maintain this important role.

The NASA STI Program Office is operated by Langley Research Center, the Lead Center for NASA's scientific and technical information. The NASA STI Program Office provides access to the NASA STI Database, the largest collection of aeronautical and space science STI in the world. The Program Office is also NASA's institutional mechanism for disseminating the results of its research and development activities. These results are published by NASA in the NASA STI Report Series, which includes the following report types:

- **TECHNICAL PUBLICATION.** Reports of completed research or a major significant phase of research that present the results of NASA programs and include extensive data or theoretical analysis. Includes compilations of significant scientific and technical data and information deemed to be of continuing reference value. NASA's counterpart of peer-reviewed formal professional papers but has less stringent limitations on manuscript length and extent of graphic presentations.
- **TECHNICAL MEMORANDUM.** Scientific and technical findings that are preliminary or of specialized interest, e.g., quick release reports, working papers, and bibliographies that contain minimal annotation. Does not contain extensive analysis.
- **CONTRACTOR REPORT.** Scientific and technical findings by NASA-sponsored contractors and grantees.

- **CONFERENCE PUBLICATION.** Collected papers from scientific and technical conferences, symposia, seminars, or other meetings sponsored or cosponsored by NASA.
- **SPECIAL PUBLICATION.** Scientific, technical, or historical information from NASA programs, projects, and missions, often concerned with subjects having substantial public interest.
- **TECHNICAL TRANSLATION.** English-language translations of foreign scientific and technical material pertinent to NASA's mission.

Specialized services that complement the STI Program Office's diverse offerings include creating custom thesauri, building customized data bases, organizing and publishing research results . . . even providing videos.

For more information about the NASA STI Program Office, see the following:

- Access the NASA STI Program Home Page at <http://www.sti.nasa.gov>
- E-mail your question via the Internet to [help@sti.nasa.gov](mailto:help@sti.nasa.gov)
- Fax your question to the NASA Access Help Desk at 301-621-0134
- Telephone the NASA Access Help Desk at 301-621-0390
- Write to:  
NASA Access Help Desk  
NASA Center for Aerospace Information  
7121 Standard Drive  
Hanover, MD 21076

NASA/TM—2001-210979



# Optimization of Training Sets for Neural-Net Processing of Characteristic Patterns From Vibrating Solids

Arthur J. Decker  
Glenn Research Center, Cleveland, Ohio

Prepared for the  
46th Annual Meeting, International Symposium on Optical Science and Technology  
sponsored by The International Society for Optical Engineering  
San Diego, California, July 29–August 3, 2001

National Aeronautics and  
Space Administration

Glenn Research Center

Available from

NASA Center for Aerospace Information  
7121 Standard Drive  
Hanover, MD 21076

National Technical Information Service  
5285 Port Royal Road  
Springfield, VA 22100

Available electronically at <http://gltrs.grc.nasa.gov/GLTRS>

# Optimization of Training Sets for Neural-Net Processing of Characteristic Patterns From Vibrating Solids

Arthur J. Decker  
National Aeronautics and Space Administration  
Glenn Research Center  
Cleveland, Ohio 44135

## ABSTRACT

Artificial neural networks have been used for a number of years to process holography-generated characteristic patterns of vibrating structures. This technology depends critically on the selection and the conditioning of the training sets. A scaling operation called folding is discussed for conditioning training sets optimally for training feed-forward neural networks to process characteristic fringe patterns. Folding allows feed-forward nets to be trained easily to detect damage-induced vibration-displacement-distribution changes as small as 10 nanometers. A specific application to aerospace of neural-net processing of characteristic patterns is presented to motivate the conditioning and optimization effort.

## 1. INTRODUCTION

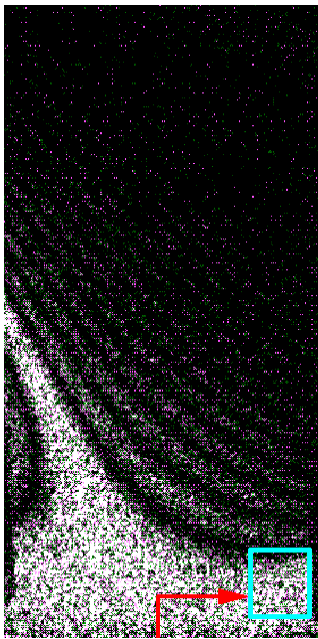
Neural-Net processing of characteristic patterns of vibrating structures is used routinely for non-destructive evaluation.<sup>1,2</sup> The characteristic patterns (Figure 1) are generated using electronic time-average holography of the vibrating structure and are sub-sampled before processing. The lower resolution patterns containing a few hundred to a few thousand pixels (Figure 2) are then presented to an experimentally trained neural network. The neural network is trained to detect small changes in the characteristic patterns resulting, for example, from structural changes or damage.

The neural-net, electronic-holography combination, used at NASA Glenn Research Center to detect structural changes and damage, has evolved through several stages. The current combination is experimentally trained; is immune to the laser speckle effect; can be used with fiber scopes; operates at 30 frames per second; and uses feed forward artificial neural networks (multi-layer perceptrons) very efficiently. The feed-forward architecture (Figure 3) is probably the most familiar architecture for so-called artificial neural networks and has much to recommend it. An artificial neural network is defined to be any processing system that is programmed with a training set of exemplars. As a specific example, the feed-forward net remains compact in software as the size of that training set increases; has good noise immunity; and can be trained with straightforward algorithms of the back-propagation genre. The feed-forward net can process fairly large input images, if the number of hidden-layer nodes is not too large, and is well suited to processing speckled characteristic patterns at 30 frames per second when those patterns contain a few hundred to a few thousand pixels.

Feed-forward artificial neural networks or multi-layer perceptrons do have a reputation at times for being unable to learn training sets that are deemed otherwise to be learnable. Research continues to be conducted in measuring the extent to which a training set is learnable.<sup>3,4</sup> Nevertheless, it has been known for some time that the performance of feed forward artificial neural networks can be enhanced greatly by conditioning the inputs. The proprietary functional-link net transforms inputs mathematically, before subjecting them to the back propagation algorithm.<sup>5</sup> Another practice that improves learning is to scale the individual pixels of the training exemplars to cover the entire input range of the feed forward net. So-called min-max tables of the minimum and maximum pixel values are used for scaling. Learning of characteristic patterns does improve with positional scaling, but the nets are susceptible to over-training.

There is a better way called *folding* to condition characteristic patterns. In *folding*, input pixels are scaled according to their locations in an intensity range rather than their positions in a characteristic pattern. *Folding* greatly increases the sensitivity of a feed-forward net for detecting changes in a characteristic pattern. This paper will discuss the learning-performance improvement achieved with *folding*.

We begin by summarizing the experimentally trained non-destructive-evaluation (NDE) method that is the motivation for improving the learning performance of the feed-forward nets. A discussion of the NDE method is used to introduce the appropriate training-record format consisting of a speckled characteristic pattern as input and a so-called degradable classification index (DCI) as output. Next, a structural model is used to create training sets containing exemplars with accurately known structural changes or damage. The training sets are then subjected to three kinds of conditioning. The conditioning consists of: the unconditioned training sets, the scaled training sets and the folded training sets. The conditioned training sets are then used to train feed-forward nets. Nets that successfully learn the training sets are tested using speckle patterns that differ from the training patterns. The relative performances of the different kinds of conditioning are compared.



**CRACK**

Figure 1: Characteristic pattern for a cracked blade.

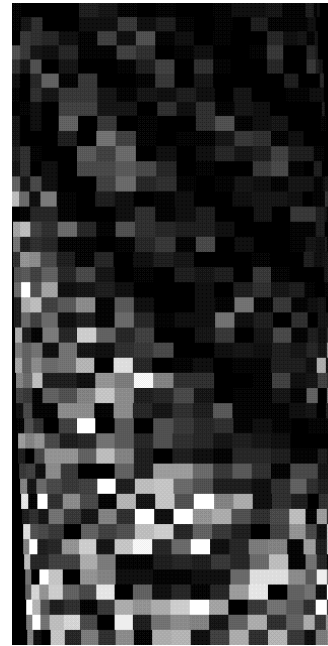


Figure 2: A sub-sampled pattern.

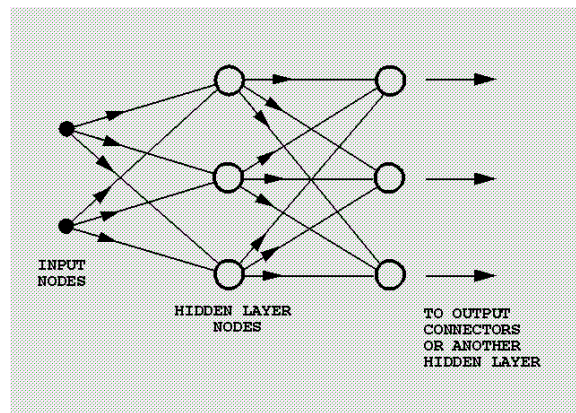


Figure 3: Feed-forward architecture.

## 2. TRAINING WITH EXPERIMENTALLY DERIVED RECORDS

### 2.1 Format of training records

A very effective experimental method has been developed for training neural networks to detect structural damage.<sup>1,2</sup> The method can be described algorithmically, and has been used to inspect an International Space Station (ISS) instrumentation cold plate for pressure-cycle induced damage. The objective of this paper is to discuss how to condition the training records to maximize the damage-detection sensitivity of this method.

A training record consists of an input and an output. The input is a characteristic pattern recorded of a vibrating structure excited to vibrate at very low amplitude. The structure is excited to vibrate in a normal or resonant mode, and the characteristic pattern shows the mode shape. A characteristic pattern is generated using electronic or television holography. Television holography is available commercially in more than one form, and is discussed extensively in the literature. Most applications use multiple holograms to average out electronic or speckle-effect noise, or to extract quantitative vibration-displacement data. The neural-net application uses only 2 holograms and consequently maintains a high sampling rate. The two holograms differ only by a  $\pi$  relative phase shift of the reference beam. The absolute value of the difference between the 2 holograms provides the visualization such as shown in fig. 1.

Training inputs actually consist of sub-sampled versions of the full TV resolution patterns such as shown in fig. 1. Sub-sampling begins by dividing the structure into large pixels. A few hundred to a few thousand large pixels are selected. Sampling is then accomplished without averaging. That is, one full-resolution pixel is recorded for each large pixel. This approach permits rapid recording of a large number of independent speckle patterns for each characteristic pattern; since there are many full-resolution pixels within a large pixel. It has been shown<sup>6</sup> that neural nets become insensitive to the details of the speckle pattern, if uncorrelated speckle patterns, equal in number to 10 percent of the number of large pixels, are used to train the net to recognize each characteristic pattern. Figure 2 shows a sub-sampled characteristic pattern of the blade in fig. 1, but at a smaller excitation amplitude.

At low frequencies, characteristic patterns or mode shapes are especially sensitive to boundary conditions and are sensitive to internal structural details and changes. The objective is to use the neural net to detect and flag such changes. The neural net uses an output to indicate the extent to which a mode has changed from a training mode as a result of structural changes or damage. The output used is a so-called degradable classification index (DCI). The DCI degrades or changes gradually as the mode shape changes from the original training shape. The DCI is encoded with 2 or 3 neural-net output nodes. The simplest example would consist of the output pair (1, 0) for a mode that was completely identical with the training mode and (0, 1) for a mode shape that differed completely from the training mode. The output would change gradually between the pairs as the mode shape changed gradually. This simple approach actually works very well, if the following algorithmic training procedure is employed.

### 2.2 Training procedure

The training and non-destructive-evaluation procedures are discussed more completely in the references.<sup>1,2</sup> The following is a brief, but useable, description. The description is reduced to an eight-step procedure.

First, select about 5 vibration modes that cover the region of interest. Figure 4 shows vibration modes covering a region of suspicious structural integrity between 4 bolt holes in an International-Space-Station (ISS) cold plate.

Second, select 3 of these modes together with the zero-amplitude condition, and collect enough independent speckle patterns for each. Figure 5 shows one speckle-pattern sample for the zero-amplitude condition. There were about 2000 large pixels for this test; hence, about 200 independent speckle-patterns-per-mode were required to train the net for speckle-pattern immunity.

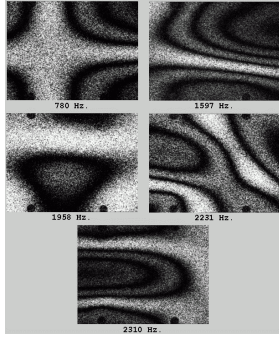


Figure 4: Modes from cold-plate.

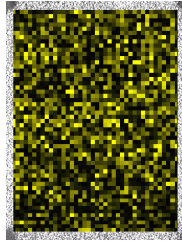


Figure 5: Sub-sampled region.

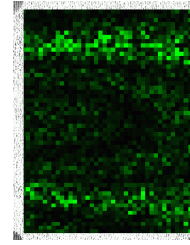


Figure 6: Mode monitored for damage.

Third, select an appropriate feed-forward neural-net architecture. The method for selecting an optimum architecture is discussed in a reference.<sup>6</sup> A 3-layer architecture is selected most often, although occasionally a 4-layer net will perform best. The input layer requires one node for each pixel. Hence, about 2000 input nodes would be required for the cold-plate example. The second layer or hidden layer contains very few nodes. It's generally desirable to use as few nodes as possible to minimize the chance of over training. Typically, 10 nodes or fewer are required. The output layer encodes the DCI and contains perhaps 2 nodes. The nodes in the hidden and output layers form a linear combination of their inputs and transform this sum non-linearly using for example a sigmoid function to generate an output. It may be necessary to transform outputs such as (1, 0) into the range [0.8, 0.2] for the sigmoid function.

Fourth, select the mode to be excited at low amplitude and monitored during a test. This mode is arbitrarily assigned the DCI (1, 0) or (0.8, 0.2). The other two modes and the zero-amplitude condition are then assigned the DCI (0, 1) or (0.2, 0.8). Figure 6 shows the sub-sampled mode that was actually monitored for the ISS cold-plate test. Only part of the mode is visible between the bolt holes.

Fifth, train the neural net to an RMS error of 0.01. The RMS error is computed from the squares of the differences between the training outputs and the measured outputs for all training records.

Sixth, define or select a value of the output node that constitutes a significant change from the training input. Environmental factors and alignment will change the DCI somewhat and randomly. A change of the large index from 0.8 to 0.7 may be considered to be significant.

Seventh, test the sensitivity of the trained net to structural changes. Typically, small point loads are applied at strategic locations on the structure, and the response of the net is noted. The design of this step is a question of structural testing rather than optical metrology. Currently, little more than the judgments of the test personnel are used to evaluate the outcome of this test.

Eighth, select a new set of vibration modes, and repeat steps one through seven, if the response of the net is not sufficiently sensitive.

The eight-step procedure has been automated with software, and a complete cycle takes about 20 minutes.

The procedure suggests at least 3 R&D questions. How do you use, quantify, or calibrate the eight-step procedure for structural NDE? How do you select a training set for optimum detection of structural changes? How do you maximize the sensitivity of a feed-forward net for learning the training set and detecting structural changes?

This paper is concerned only with maximizing sensitivity, but structural finite element models can be used in part to formulate answers to all three questions. We shall use finite-element-model-generated training sets to investigate the conditioning of inputs to optimize the training of feed-forward nets. These training sets are described in the next section.

### 3. MODEL-GENERATED TRAINING SETS FOR CHECKING CONDITIONING TECHNIQUES

Structural finite-element models have been combined with a model of the laser speckle effect and a model of electronic holography to generate characteristic patterns, and these patterns have been used to train artificial neural networks. The practice has had limited success. Neural nets trained with a cantilever model were able to detect damage in a physical cantilever.<sup>7</sup> But neural nets trained with characteristic patterns generated from deterministic finite-element models of twisted fan blades have been unable to recognize or detect damage in the physical fan blades.<sup>8,9</sup> The calculated characteristic patterns are too sensitive to boundary conditions and to sample-particular structural properties to represent real structures accurately enough for our NDE method.

Nevertheless, this paper assumes, supported by the success of the cantilever example, that model-generated *changes* in patterns are sufficiently realistic to be used to test the effectiveness of input conditioning on neural-net training. A model is used to generate vibration displacement distributions for undamaged and cracked twisted blades. The size of the crack effect is varied to check sensitivity. The displacement distributions are combined with models of electronic holography and the laser speckle effect to generate characteristic patterns. These characteristic patterns can then be transformed in various ways to measure the effects of input conditioning on neural-net training and sensitivity.

The model is discussed in the references<sup>8,9</sup>, and the features needed to understand the training sets are summarized briefly here. Both cantilever and twisted-blade models have been used to investigate the effects of conditioning, but this study will be confined to a twisted-blade model. The blade and finite-element node pattern are shown in fig. 7. Figure 1 shows a characteristic pattern and fig. 2 shows a sub-sampled pattern from the twisted blade. The blade geometry is of constant cross-section and has a twist that varies linearly from 0 degrees at the root to 30 degrees at the tip. Blade dimensions are chord, 8.72 cm (3.433 in); maximum thickness to chord ratio, 0.037; and span, 15.24 cm (6.0 in). The finite element models have a 20x42 mesh of quadrilateral elements along the mid-thickness of the airfoil section. The finite element model (MSC/NASTRAN Solution 103) tabulates relative vector displacements at 21x43 finite-element nodes. Only the lowest frequency mode predicted at 199 Hz was used for this study. The blade material for this prediction was 6061-T6 Aluminum with a Young's Modulus of 66.19 Gpa ( $9.6 \times 10^6$  psi), a Poisson's Ratio of .33, and a Mass Density of 2712.832 kg/m<sup>3</sup> ( $2.536 \times 10^{-4}$  lbf sec<sup>2</sup>/in<sup>4</sup>).

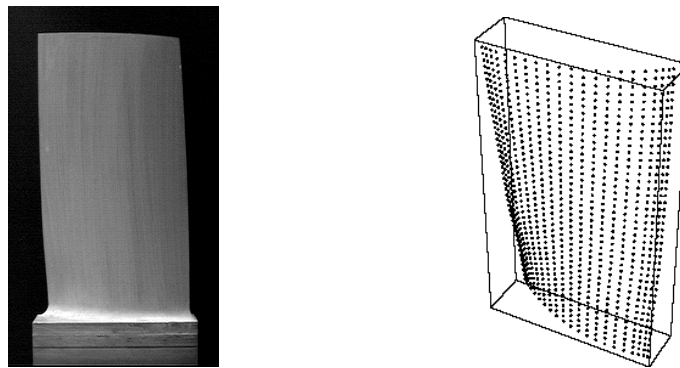


Figure 7: Blade and finite-element node-pattern used for model.

Two finite element models were generated, one with a simulated crack and the other without. The crack is located at the root and extends from 87% to 100% of chord. The blades were structurally modeled as cantilevers by constraining the root nodes in all six degrees of freedom, except in the simulated crack region. The crack was simulated by releasing the constraints for all degrees of freedom at the nodes in the crack's region.

Another feature called a crack-effect amplification factor  $f$  was added only to check optical sensitivity. The change in displacement distribution between the cracked and undamaged blades is multiplied by this factor. When  $f=1$ , the model is used as is. When  $f > 1$ , the optical effect of the crack is greater than predicted by the finite element model. When  $f < 1$ , the optical effect of the crack is less than predicted by the finite element model.

The finite element model must be combined with 2 optical effects. First, the laser speckle effect must be modeled. The simplest model was chosen where the real and imaginary parts of the object-beam amplitude were normally distributed.

Random number generators assured uncorrelated speckle patterns. Second, a sensitivity vector  $\mathbf{K}$  (equation 1) must be included for the holography process. The sensitivity vector can be unfavorable for parts of a highly twisted blade, but has little effect on the blade used for this study.

The model was used to generate one pixel for each point at which the displacement was tabulated. A complication evident in fig. 7 is that the points are non-uniformly placed. This effect is specifically handled by our software and measurements.

A final comment is that calculated holograms of both the whole blade and a zoomed region have been used for past tests. The zoomed displacement distributions were often required during previous work to generate adequate sensitivity, and were generated by cubic interpolation of the finite-element model. This study is confined to the whole blade. The next section discusses the transformation of input characteristic patterns to improve neural-net sensitivity.

#### 4. TRANSFORMATIONS OF CHARACTERISTIC PATTERNS

The raw input data actually is a signed, speckled pattern, or cross-interference term, whose individual pixels satisfy the expression

$$\text{pixel value} = A \cos[\theta] J_0[2\pi\mathbf{K}\cdot\boldsymbol{\delta}] \quad (1)$$

where  $A$  is a positive random quantity;  $\theta$  is random variable uniformly distributed from  $0$  to  $2\pi$ ;  $J_0$  is the Bessel function of the first kind and zero order;  $\mathbf{K}$  is the sensitivity vector; and  $\boldsymbol{\delta}$  is the vibration displacement amplitude measured in wavelengths of light.

Many transformations of this quantity are possible, but the practice for a long time was to take the absolute value. Then pixel values could be arranged from  $0$  to  $255$  for visualization. The same absolute values were used to train the neural networks as well.

It was conjectured, of course, that taking the absolute value might eliminate information whose loss might degrade the learning and sensitivity of the neural networks. But the surprising finding was that feed-forward nets trained with the signed quantity were harder to train than nets trained with the absolute value. A hyperbolic tangent function is used rather than a sigmoid function for signed inputs. Figure 8 shows that the absolute-value transformation is a folding operation about zero intensity. In relative terms, intensities in the range  $[-1, 0)$  are transformed into the range  $[1, 0)$ , and intensities in the range  $[0, 1]$  are transformed identically to  $[0, 1]$ . It was recognized that this symmetrical process could be continued. For example, figure 9 shows a transformation of  $[-1.0, -0.5]$  into the range  $[1.0, 0]$ , a transformation of  $[-0.5, 0]$  into the range  $[0, 1.0]$ , a transformation of  $[0, 0.5]$  into the range  $[1.0, 0]$ , and a transformation of  $[0.5, 1.0]$  into the range  $[0, 1.0]$ . It was discovered that feed-forward nets trained with this folded data learned more easily than nets trained with the absolute value, and that learning can improve as the number of folds increases.

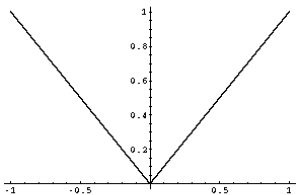


Figure 8: 1 fold or absolute value.

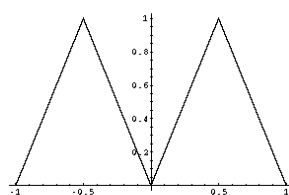


Figure 9: 3 folds with normal contrast.

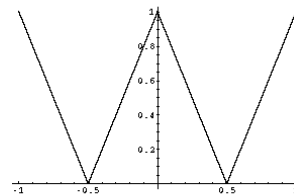


Figure 10: 3 folds and reversed contrast.

*Folding* can be made non-symmetrical and non-uniform, but this paper will cover the symmetrical and uniform case only. The symmetrical case requires that the number of folds  $N$  be odd. Here  $N=0$  corresponds to unfolded, signed characteristic patterns and  $N=1$  corresponds to the absolute value. Figure 9 has  $N=3$ . Folding can also be accompanied

by a contrast reversal as in figure 10. In general, we shall define transformations in which dark fringes remain dark as having normal contrast. Normal contrast requires that zero intensities be transformed to zero.

*Folding* is an intensity dependent transformation. For comparison, we shall use another transformation called a min-max table. For a min-max table, all the intensities in the training set at each point in the characteristic pattern are tabulated. The difference between the minimum and maximum intensities at each point is then used to scale the data into the full input range of the neural network. That range typically is [0.2, 0.8] for a feed-forward net that uses a sigmoid transfer function. The min-max table, unlike folding, will scale even a dark fringe into the full input range of the neural network.

The next section presents results that show the performance improvement afforded by *folding*.

## 5. RESULTS USING TRANSFORMED TRAINING RECORDS

Training sets were generated for maximum vibration amplitudes of 1.0 wave, 5.0 waves and 64.0 waves, and for crack-effect amplification factors  $f=1.0$  and  $f=0.1$ . Recall that  $f=1.0$  refers to the model-generated cracks, and  $f=0.1$  refers to crack effects 10 times smaller. One wave equals 1 wavelength of light. Training and test sets were generated for 0, 1, 3, 5, 7, and 9 folds, where  $N=0$  represents the signed, unfolded data. The training and tests sets have uncorrelated speckle patterns. The  $N=0$  case was also used to train a net with min-max scaling for comparison.

The same neural-net architecture was used for all tests. The feed-forward neural network had an input layer containing 903 nodes, a hidden layer containing 5 nodes and an output layer containing 3 nodes to encode the DCI. One of the 3 output nodes is intended as a no-decision indicator, but was not used for this study, where it was clamped to 0.2. The nets were always trained with 11,000 back-propagation iterations. After training, RMS errors were measured for both the training and test sets. The identification error rate was also noted. An identification error was declared, if the maximum node indicated an output below 0.6. Note that the training value of a maximum node is 0.8. The DCI triple (0.8, 0.2, 0.2) was used as the training value for the undamaged case, and the DCI triple (0.2, 0.2, 0.8) was used as the training value for the cracked case.

Figure 11 clearly shows the effectiveness of *folding* in improving the performance of a feed-forward neural network. Figure 11 was generated for an amplitude of 5.0 waves and a crack-effect amplification factor  $f=0.1$ . The net does not train at all until there are 7 folds, and the 9-fold case performs better than the 7-fold case.

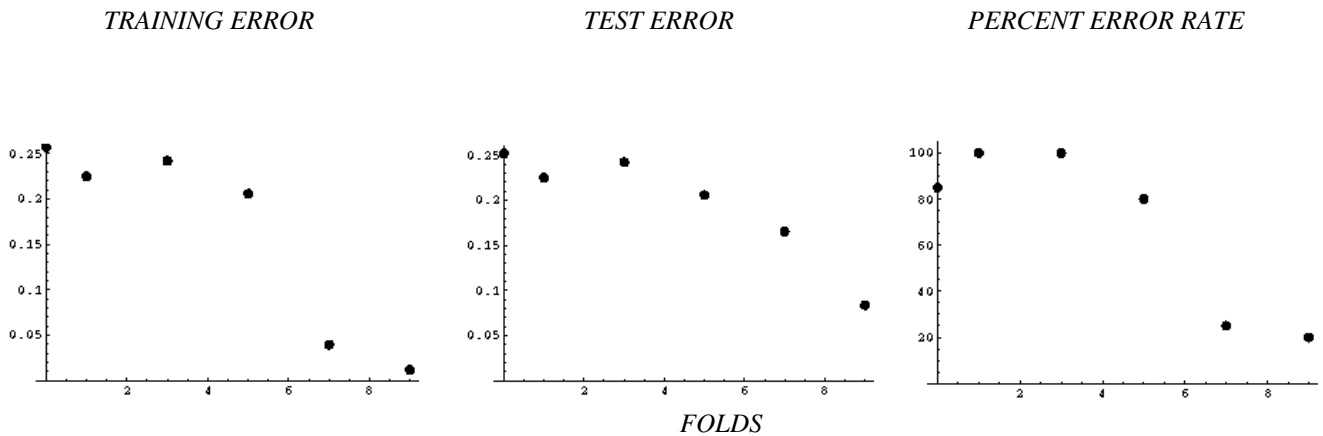


Figure 11: Performance of *folding* for an excitation amplitude of 5.0 waves and a crack-effect amplification  $f=0.1$ .

The same result pertains to other combinations of crack-effect amplification and vibration amplitude. Figure 12 shows the result for an amplitude of 1.0 wave and a crack-effect amplification factor  $f=1.0$ . Nine folds are required here for a 0% error rate; however the error rate is down to 5% at 3 folds.

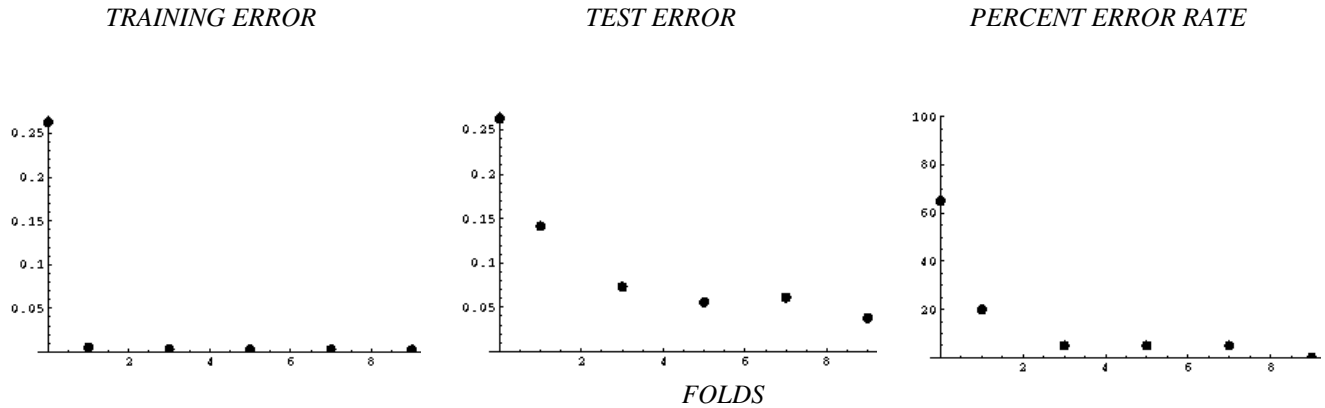


Figure 12: Performance of *folding* for an excitation amplitude of 1.0 wave and a crack-effect amplification  $f=1.0$ .

In general, the performance of the feed-forward net improves for large vibration amplitudes. Figure 13 shows the result for an amplitude of 64.0 waves and a crack-effect amplification factor  $f=1.0$ . All folded examples perform adequately at the higher amplitude.

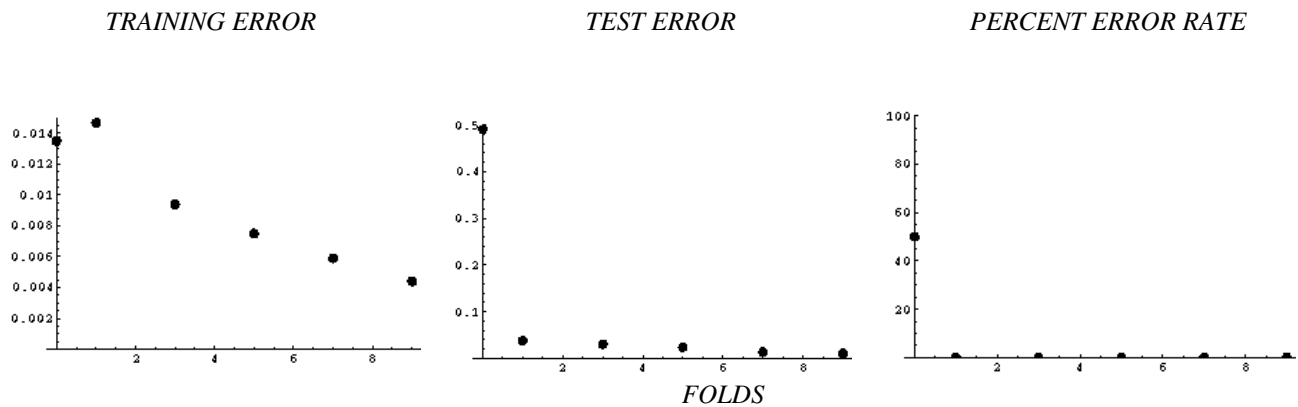


Figure 13: Performance of *folding* for an excitation amplitude of 64.0 waves and a crack-effect amplification  $f=1.0$ .

In general, the unfolded case ( $N=0$ ) does not perform well or even adequately. Furthermore, min-max table scaling does not help. Min-max scaling of the 64.0 wave,  $f=1.0$  case yields a training error of 0.036, a test error of 0.9916, and an error rate of 80 percent.

## 6. DISCUSSION OF RESULTS

Figure 11 clearly shows, not only that *folding* improves the performance of the feed-forward neural network, but also that *folding* is absolutely essential for training in some cases. Neither the unsigned characteristic pattern ( $N=0$ ), nor the absolute value ( $N=1$ ) used most often for training the nets in the past, were able to train the net for fig. 11.

A natural question arises. Just how sensitive is the feed-forward-net, folding combination for detecting structural changes? This paper can provide an answer only for the model-generated characteristic patterns and model-calculated damage reported herein. That damage refers specifically to a crack at 0 span. Nevertheless, the results are reasonably impressive. A net was trained for  $f=0.01$  and a vibration amplitude of 64.0 waves. Nine folds ( $N=9$ ) were employed. The net was allowed to develop a minimum RMS training error of 0.01. The test RMS error was fairly high (0.2504), but the actual identification error rate was only 20 percent. The large test error was contributed mainly by values of the large node greater than 0.8, resulting still in largely correct identifications. Hence, this net, training-set combination probably was performing at the limit of detection. A symptom of impending net failure is an increasing test-error. Complete failure occurs when the

training error increases to a large value. The damage detected would have produced a maximum change in the displacement distribution of less than 10 nanometers in an experimental test.

A final comment is that holography actually detects the dot product of the sensitivity vector and the displacement vector as shown in equation (1). This paper used a distribution of the sensitivity vector characteristic of a typical setup in a NASA Glenn holography laboratory used to inspect the physical fan blade whose model was used for this study. The minimum dot-product effect was still about 95 percent of the maximum possible effect, mainly because most of the motion was in the direction of the optical axis.

## 7. CONCLUDING REMARKS

The conclusion is that *folding* greatly improves the performance of feed-forward nets for learning speckled characteristic-pattern training records and is absolutely essential for learning to differentiate training records corresponding to small structural changes. Vibration-displacement-distribution changes as small as 10 nanometers can be detected at the maximum-difference point.

Future work pertains mainly to non-destructive evaluation and structural analysis practices. There is a need to quantify and calibrate the inspection method discussed in Section 2 and to render it consistent with NASA standards. It would also be interesting to measure the susceptibility-to-learning of the characteristic-pattern training records independently of the neural-net architecture.

## 8. REFERENCES

1. A. J. Decker, M. E. Melis and K. E. Weiland, "Inspection of Space Station Cold Plate Using Visual and Automated Holographic Techniques," *NASA/TM—1999-209388*, Aug. 1999.
2. A. J. Decker, "Neural-Net Processed Characteristic Patterns for Measurement of Structural Integrity of Pressure Cycled Components," *Proceedings of JANNAF, 12<sup>th</sup> Nondestructive Evaluation Subcommittee*, Cocoa Beach, Florida, 26-30 March 2001.
3. M. T. Manry, S. J. Apollo and Q. Yu, "Minimum Mean Square Estimation and Neural Networks," *Neurocomputing* **13**, pp. 59—74, 1996.
4. M. T. Manry, et al., "Cramer Rao Maximum A-Posteriori Bounds on neural Network training Error for Non-Gaussian Signals and Parameters," *International Journal of Intelligent Control and Systems* **1**, pp. 381-391, 1996.
5. Yoh-Han Pao, *Adaptive Pattern Recognition and Neural Networks*, chapter 8, Addison-Wesley, New York, 1989.
6. A. J. Decker, E. B. Fite, O. Mehmed and S. A. Thorp, "Processing speckle patterns with model trained neural networks", *Optical Technology in Fluid, Thermal, and Combustion Flow III, Proc. SPIE*, S. S. Cha, J. D. Trolinger and M. Kawahashi, eds., **vol. 3172**, pp. 285-293, 1997.
7. A. J. Decker, E. B. Fite, O. Mehmed and S. A. Thorp, "Vibrational Analysis of Engine Components Using Neural-Net Processing and Electronic Holography," *Advanced Non-Intrusive Instrumentation for Propulsion Engines, AGARD-CP-598*, pp. 33-1--33-6, 1998.
8. A. J. Decker, E. B. Fite, S. A. Thorp and O. Mehmed, "Comparison of computational-model and experimental-example trained neural networks for processing speckled fringe patterns," *International Conference on Optical Technology and Image Processing Fluid, Thermal, and Combustion Flow, Proceedings of VSJ-SPIE '98, on compact disc in pdf, paper AB002*, 1998.
9. A. J. Decker, "Neural-Net Processing of Characteristic Patterns," *Topics on Nondestructive Evaluation Series, Automation, Miniature Robotics and Sensors for Nondestructive Evaluation and Testing*, Yoseph Bar-Cohen, Technical Editor, **vol. 4**, chapter 7.1, The American Society for Nondestructive Testing, Inc., 2000.

<b>REPORT DOCUMENTATION PAGE</b>			<i>Form Approved</i> <i>OMB No. 0704-0188</i>	
Public reporting burden for this collection of information is estimated to average 1 hour per response, including the time for reviewing instructions, searching existing data sources, gathering and maintaining the data needed, and completing and reviewing the collection of information. Send comments regarding this burden estimate or any other aspect of this collection of information, including suggestions for reducing this burden, to Washington Headquarters Services, Directorate for Information Operations and Reports, 1215 Jefferson Davis Highway, Suite 1204, Arlington, VA 22202-4302, and to the Office of Management and Budget, Paperwork Reduction Project (0704-0188), Washington, DC 20503.				
<b>1. AGENCY USE ONLY (Leave blank)</b>		<b>2. REPORT DATE</b> July 2001	<b>3. REPORT TYPE AND DATES COVERED</b> Technical Memorandum	
<b>4. TITLE AND SUBTITLE</b>  Optimization of Training Sets for Neural-Net Processing of Characteristic Patterns From Vibrating Solids			<b>5. FUNDING NUMBERS</b>  WU-323-78-00-00	
<b>6. AUTHOR(S)</b>  Arthur J. Decker				
<b>7. PERFORMING ORGANIZATION NAME(S) AND ADDRESS(ES)</b>  National Aeronautics and Space Administration John H. Glenn Research Center at Lewis Field Cleveland, Ohio 44135-3191			<b>8. PERFORMING ORGANIZATION REPORT NUMBER</b>  E-12833	
<b>9. SPONSORING/MONITORING AGENCY NAME(S) AND ADDRESS(ES)</b>  National Aeronautics and Space Administration Washington, DC 20546-0001			<b>10. SPONSORING/MONITORING AGENCY REPORT NUMBER</b>  NASA TM-2001-210979	
<b>11. SUPPLEMENTARY NOTES</b>  Prepared for the 46th Annual Meeting, International Symposium on Optical Science and Technology sponsored by The International Society for Optical Engineering, San Diego, California, July 29-August 3, 2001. Responsible person, Arthur J. Decker, organization code 5520, 216-433-3639.				
<b>12a. DISTRIBUTION/AVAILABILITY STATEMENT</b>  Unclassified - Unlimited Subject Category: 35 Available electronically at <a href="http://gltrs.grc.nasa.gov/GLTRS">http://gltrs.grc.nasa.gov/GLTRS</a> This publication is available from the NASA Center for AeroSpace Information, 301-621-0390.			<b>12b. DISTRIBUTION CODE</b>	
<b>13. ABSTRACT (Maximum 200 words)</b>  Artificial neural networks have been used for a number of years to process holography-generated characteristic patterns of vibrating structures. This technology depends critically on the selection and the conditioning of the training sets. A scaling operation called folding is discussed for conditioning training sets optimally for training feed-forward neural networks to process characteristic fringe patterns. Folding allows feed-forward nets to be trained easily to detect damage-induced vibration-displacement-distribution changes as small as 10 nm. A specific application to aerospace of neural-net processing of characteristic patterns is presented to motivate the conditioning and optimization effort.				
<b>14. SUBJECT TERMS</b>  Holography; Neural networks; Characteristic patterns			<b>15. NUMBER OF PAGES</b> 15	
			<b>16. PRICE CODE</b>	
<b>17. SECURITY CLASSIFICATION OF REPORT</b> Unclassified	<b>18. SECURITY CLASSIFICATION OF THIS PAGE</b> Unclassified	<b>19. SECURITY CLASSIFICATION OF ABSTRACT</b> Unclassified	<b>20. LIMITATION OF ABSTRACT</b>	